ELSEVIER

Thermochimica Acta 304/305 (1997) 179–186

thermochimica acta

Investigation of polymer melting by temperature modulated differential scanning calorimetry and it's description using kinetic models

J.E.K. Schawe[a,*], E. Bergmann[b]

[a] *Universität Ulm, Sektion für Kalorimetrie, D-89069 Ulm, Germany*
[b] *IFA Privates Institut für angewandte Analysentechnik GmbH, Schillerstr. 18, D-89077 Ulm, Germany*

Received 27 March 1997; accepted 23 August 1997

Abstract

Using temperature modulated differential scanning calorimetry (TM-DSC) the complex frequency dependent heat capacity $C(\omega)$ can be measured. $C(\omega)$ is connected to an additional time dependent variable $\zeta(t)$, which describes the kinetics of processes inside the sample. Usage of phenomenological or molecular models for $\zeta(t)$ allows the interpretation of measured TM-DSC curves. This is illustrated for the melting of Poly(ethylene terephthalate) (PET) and Poly(E-caprolactone) (PCL).

The melting of polymers is investigated and compared to a first- and second-order phase transition. The behaviour of the complex heat capacity in the melting region of polymers is manifold. Using different empirical models for the local melting and relaxation process in the melt the quantitative behaviour of the measured curves can be described. © 1997 Elsevier Science B.V.

Keywords: Heat capacity; Kinetics; Polymer melting; Temperature modulated differential scanning calorimetry (TMDSC)

1. Introduction

TM-DSC applies a periodical temperature modulation at a conventional DSC run [1,2]. Dependent on the instrumentation different methods of modulation and analyses are available [3,4]. The heat flow amplitude and the phase shift φ between scanning rate modulation and heat flow can be determined [5] from the periodic component of the measured heat flow rate. The application of these properties for interpretations is established in glass transition [6–9] as well as in polymer crystallisation [10,11].

Here we present results of investigations of polymer melting using TM-DSC. The melting behaviour of polymers is compared to first- and second-order phase transition. Based on the thermodynamic description of TM-DSC measurements [12,13] different kinetic models for melting processes are investigated.

2. Theoretical description of TM-DSC signals

A detailed description of TM-DSC signals using linear response approach is given in Refs. [12,13]. Here we give only a short introduction.

In case of TM-DSC the measured signal is the heat flow rate Φ. It is separated into an underlying and a periodic component:

$$\Phi(t) = \Phi_u(t) + \Phi_p(t) \quad (1)$$

*Corresponding author.

PII S0040-6031(97)00187-1

where the linear underlying scanning rate β_0 yields the underlying component Φ_u, and the periodic term (with the temperature amplitude T_a and the angular frequency $\omega_0 = 2\pi/t_p$; t_p is the period) for the periodic component Φ_p. The underlying component is related to the conventional DSC curve:

$$\Phi_u = C_\beta \beta_0 \tag{2}$$

where C_β is the (heating rate dependent) heat capacity and a part which depends on the latent heat.

A common separation method of Φ_u and Φ_p on the measured heat flow rate is the Fourier analysis and subtraction. The first harmonic of the periodic heat flow component is:

$$\Phi_{p1}(t) = \Phi_a(t)\cos(\omega_0 t - \varphi) \tag{3}$$

where Φ_a is the amplitude of the heat flow rate and φ is the phase shift between the heating rate $\beta = dT/dt$ and the heat flow rate Φ_{p1}. After calibration of amplitude and phase [14,15] the complex heat capacity

$$C(\omega) = C'(\omega) - iC''(\omega) \tag{4}$$

can be calculated from the measured curve. The real part C' describes the component in phase with the heating rate and the imaginary part C'' the component out-of-phase. If time dependent processes takes place in the sample, the imaginary component of the heat capacity will appear. These processes can be described by irreversible thermodynamics. In this case an additional time dependent variable ζ must be introduced. The total differential of the entropy for isobaric conditions reads

$$dS = \left(\frac{\partial S}{\partial T}\right)_{p,\zeta} dT + \left(\frac{\partial S}{\partial \zeta}\right)_{p,T} d\zeta = dS_e + dS_i \tag{5}$$

where dS_e is the entropy change of the system due to exchange of heat and dS_i is the additional internal entropy change due to irreversible processes.

We can define the generalised isobaric heat capacity as

$$C(T,t) = T\left(\frac{dS(T,t)}{dT}\right) = T\left(\frac{\partial S}{\partial T}\right)_{p,\zeta} + T\left(\frac{\partial S}{\partial \zeta}\right)_{p,T} \frac{d\zeta(t)}{dT} \tag{6}$$

The first term represents the static part of the heat capacity C_{st}, it represents the very fast thermal motions in solids (the characteristic frequency is in the range of 10^{10} Hz). The second term in Eq. (6) describes the time dependent part $C_{dyn}(T,t)$:

$$C(T,t) = C_{st}(T) + C_{dyn}(T,t) \tag{7}$$

C_{dyn} represents all relative slow processes in the sample. In the following the temperature change is assumed to be so small that the heat capacity is not a function of temperature.

In a TM-DSC measurement the frequency dependent heat capacity $C(\omega)$ is measured. The connection between $C(\omega)$ and the time dependent heat capacity $C(t)$ is given by Fourier transform:

$$C(\omega) = C_{st} + \int_0^\infty \dot{C}_{dyn}(t')e^{-i\omega t'}dt' = C_{st} + (C'_{dyn}(\omega) - iC''_{dyn}(\omega)) \tag{8}$$

where $\dot{C}_{dyn} = dC_{dyn}/dt$. Comparing Eqs. (8) and (4) yields:

$$C'(\omega) = C_{st} + C'_{dyn}(\omega) \tag{8a}$$

$$C''(\omega) = C''_{dyn}(\omega) \tag{8b}$$

The correspondence between the measured entropy change and the heat capacity is given by the convolution product [12]:

$$T\Delta S = C_{st}\Delta T(t) + \frac{d}{dT}\int_{-\infty}^{t} C_{dyn}(t-t')\Delta T(t')dt' \tag{9}$$

For investigation of the connection between the order parameter $\zeta(t)$ and the heat capacity we discuss the response of the sample to a small temperature step:

$$\Delta T(t) = \Delta T_0 \Theta(t) \tag{10}$$

where ΔT_0 is the small step height and $\Theta(t)$ the step function. In this case for the entropy production from Eq. (5) reads:

$$\frac{dS_i}{dt} = \left(\frac{dS}{d\zeta}\right)_{p,T} \dot{\zeta}(t) \tag{11}$$

By inserting of Eqs. (10) and (5) in Eq. (9) follows:

$$\Delta S_i = C_{dyn}(t)\frac{\Delta T_0}{T} \tag{12}$$

Thus the entropy production is:

$$\frac{dS_i}{dt} = \dot{C}_{dyn}(t)\frac{\Delta T_0}{T} \tag{13}$$

A comparison of Eqs. (11) and (13) shows the connection between ζ and C:

$$\dot{C}_{dyn}(t) \propto \dot{\zeta}(t) \tag{14}$$

The proportional factors is

$$\left(\frac{dS}{d\zeta}\right)_{p,T}\frac{T}{\Delta T_0}.$$

The variable ζ describes the kinetics of the process. In the following paragraphs the results of different approaches for ζ shall be compared with measured melting curves of polymers.

3. Experimental investigation and results

The melting behaviour of poly(ethylene terephthalate) (PET; $M_w = 23.000$) and poly(E-caprolactone) (PCL) was investigated using a Perkin-Elmer DSC-7 in the DDSC mode. This instrument does not allow the selection of an underlying heating rate, modulation amplitude and modulation frequency. However, if desired, such quantities may be determined after the fact, once the heating and cooling ramps which make up the thermal program have been selected. The used calibration procedure is described elsewhere [15].

Before discussing the polymer melting curves a first-order transition (melting of Indium; In) and a second-order transition (transition at 275°C of sodium nitrate; $NaNO_3$) will be investigated.

3.1. First- and second-order phase transitions

For the measurements of a pure first-order transition a 7.808 mg In sample was used. The second melting was investigated. The experimental parameters were: $\beta_0 = 0.025$ K/min, $T_a = 0.005$ K and $t_p = 48$ s. The result is shown in Fig. 1. With these parameters approximately 12 periods of modulation occur in the melting region.

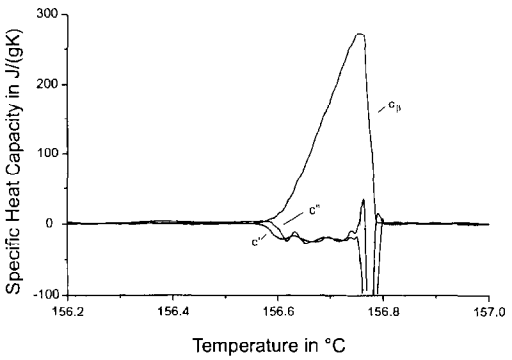

Fig. 1. The specific heat capacity functions for the first-order melting of indium by TM-DSC ($m = 7.808$ mg, $\beta_0 = 0.025$ K/min, $T_a = 0.01$ K, $t_p = 48$ s).

A first-order transition is characterised by a transition temperature and an enthalpy of fusion. The theoretical heat flow curve is a Dirac function. In a conventional DSC the maximal heat flow into the sample is limited by the thermal resistor between sample and furnace. During the melting the sample temperature remains constant and the respective heat flow rate curve in a conventional DSC shows a constant slope during the transition. The reason of this behaviour is that the temperature is not measured in the sample but only in the furnace close to the sample. Therefore, the heat transfer affects the measured curves. If the sample is completely molten, then the sample temperature increases again. In the TM-DSC we find this curve type in the underlying signal C_β. Calculations concerning the influence of heat transfer on the DSC signal in the melting region show that during the melting the 'apparent heat capacity' drops down because of latent heat [16]. C' and C'' do not reflect the properties of the sample in case of a first-order phase transition, but describe the measured heat flow caused by heat transfer. At such a transition the complex heat capacity characterises only the changes of the heat transfer conditions inside the DSC furnace.

For investigation of the signal behaviour during a second-order transition we used the solid-state transition at 275°C of $NaNO_3$ [17]. The 8.796 mg sample was measured at a period of 48 s, an underlying heating rate of 0.125 K/min and a temperature amplitude of 0.055 K. The respective complex heat capacity is shown in Fig. 2. This transition has a distinct influence on the C' signal. At temperatures, below

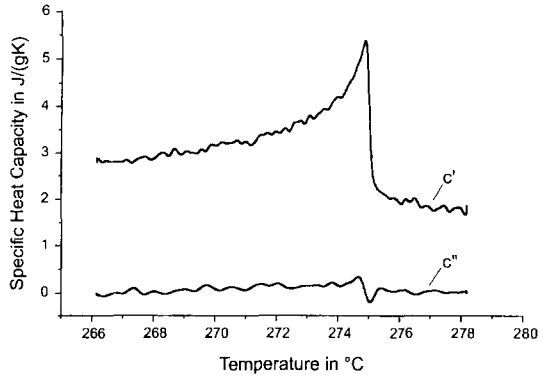

Fig. 2. The specific complex heat capacity for the second-order solid state transition of $NaNO_3$ ($m = 8.786$ mg, $\beta_0 = 0.125$ K/min, $T_a = 0.055$ K, $t_p = 48$ s).

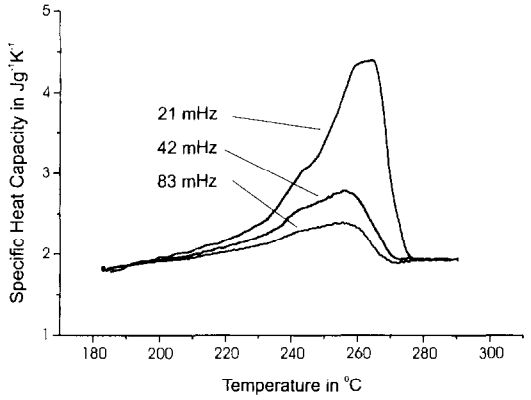

Fig. 3. Real part of the specific heat capacity in the melting region of PET at different frequencies. ($m = 4.324$ mg, $\beta_0 = 1$ K/min, $T_a = 0.2$ K).

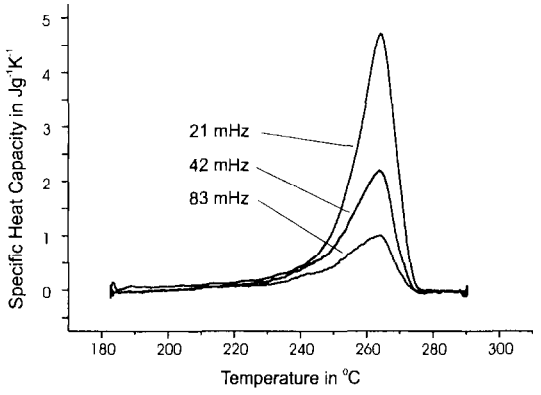

Fig. 4. Imaginary part of the specific heat capacity in the melting region of PET (same conditions as in Fig. 3).

the critical temperature the heat capacity C' increases. After the critical temperature, the heat capacity drops back. This corresponds to the expected behaviour of the heat capacity in the transition region. During this type of transition C'' is approximately zero.

3.2. Polymer melting

Before measurement the molten PET sample ($m = 4.324$ mg) was quenched to the crystallisation temperature ($T_c = 170$°C). The crystallisation time was 30 min. The partial crystalline sample was measured using an underlying heating rate $\beta_0 = 1$ K/min and a temperature amplitude $T_a = 0.2$ K. The frequency was varied between 10 and 83 mHz. In Figs. 3 and 4 some results are shown. The real as well as the imaginary part of heat capacity is positive. The peak height is frequency dependent. For the imaginary part of heat capacity, both the peak width and the maximum temperature are frequency independent. The peak form of the real part of the heat capacity C' depends, however, on frequency. Even at relatively low temperatures (lower than 220°C) the C'-curve increases, whereas the C''-curve is approximately constant in this temperature range. The maximum temperature of the C'-peak is at lower temperatures as the C''-peak maximum. The form of the C''-curves shows a good correspondence to the peak of the underlying signal (or the conventional DSC-curve).

The melting behaviour of PCL is investigated with a 4.380 mg sample. Before each measurement the sample was cooled from the melt at 70 to 25°C with 50 K/min. Afterwards the sample was partially crystalline. The experimental parameters for the TM-DSC measurements are $\beta_0 = 0.2$ K/min and $T_a = 0.1$ K. The chosen periods are 30, 48, 60 and 96 s (f_0 : 33, 21, 17 and 10 mHz, respectively). In Figs. 5 and 6 the heat capacity curves are shown. In correspondence to the results of PET the imaginary part C'' of PCL shows a positive peak in the melting region. The peak height decreases with increasing frequency. This peak sharp is similar to the C_β-peak. In contrast to PET, the C'-curves of PCL show a small exothermic, which is also frequency dependent.

A problem at interpretation of TM-DSC curves in the melting range of polymers is the insufficient

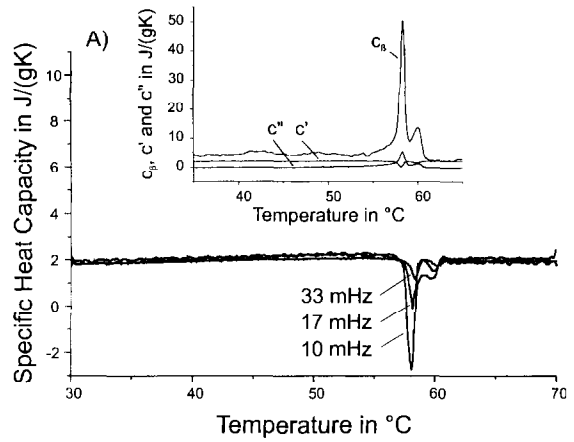

Fig. 5. Real part of the specific heat capacity in the melting region of PCL at different frequencies. ($m = 4.380$ mg, $\beta_0 = 0.2$ K/min, $T_a = 0.1$ K). Insertion (A) shows the complete set of specific heat capacities measured at 17 mHz.

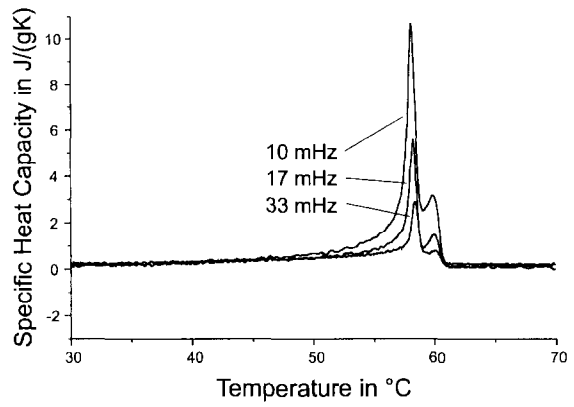

Fig. 6. Imaginary part of the specific heat capacity in the melting region of PCL (same conditions as in Fig. 5).

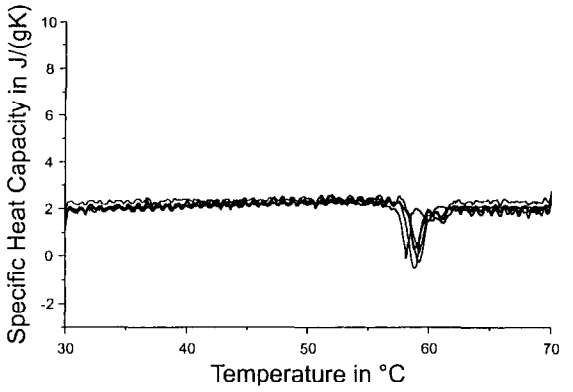

Fig. 7. Real part of the specific heat capacity in the melting region of PCL measured at different sample masses (sample masses: 1.664 (two measurements) 2.948, 4.380, 6.330 mg, $f = 17$ mHz, $\beta_0 = 0.2$ K/min, $T_a = 0.1$ K).

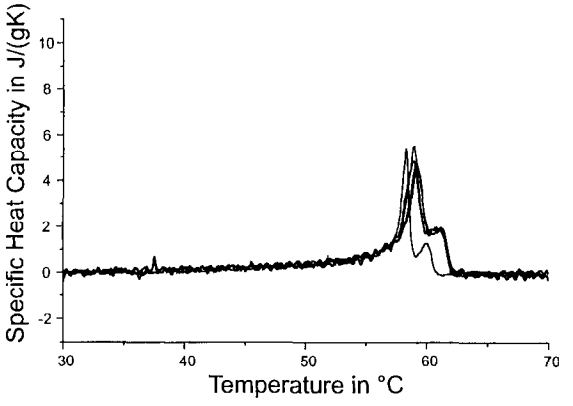

Fig. 8. Imaginary part of the specific heat capacity in the melting region of PCL (same conditions as in Fig. 7).

number of reliable measuring results. Therefore it seems to be possible that the results in Figs. 3 and 6 are caused by heat transfer. One possibility to check this is a variation of the sample mass. If the measured effects characterise real processes in the sample the intensity of the complex heat capacity should be independent of the sample mass. To investigate the influence of the sample mass on the measured signal four PCL samples (1.664, 2.948, 4.380 and 6.330 mg) are investigated at a frequency of 17 mHz and an underlying heating rate of 0.5 K/min. Both the real and the imaginary part of the complex heat capacity are shown in Figs. 7 and 8. Fig. 9 shows the heights of the c' and c''-peak, respectively. These figures do not show a dependence of the sample mass. Differences in the curves results on the chemical and structural irregularities of the samples (i.e. the influence of water, different crystallinity, etc. on the melting behaviour). For that reason, we proceed to take kinetic processes during the polymer melting into account as occasion for the form of the measured curves.

Obviously different polymers show different behaviour of the complex heat capacity in the melting

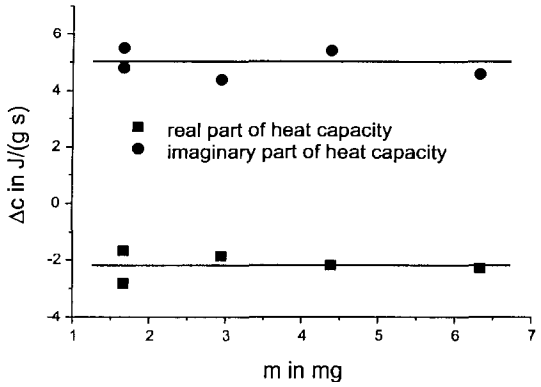

Fig. 9. The heights of the measured c' and c'' peaks as function of the sample mass (determined from Figs. 7 and 8).

region. Both investigated materials differ from first- and second-order phase transition. In contrast to such phase transitions the polymers shows a relatively large peak in C'' and a frequency dependent exothermic or endothermic in C'. The occurrence of a C'' signal and the frequency dependence of the complex heat capacity in the melt region of polymers point to the importance of kinetic processes. In contrast to the cold crystallisation of polymers the melting should take place not so far from the equilibrium. This means that during melting the entropy of the melt in the neighbourhood of the melting front should not be very different from that of the crystal. Therefore a relaxation of the entropy occurs. In this case the linear response yields information about the kinetics of the processes, which take place during melting.

4. Models for description of the TM-DSC signals if polymer melting

In the following empirical models for the time dependent internal variable ζ are discussed. In this sense ζ is interpreted as an order parameter, it describes the crystallinity of the sample. In this context the time derivative $d\zeta/dt$ is proportional to the rate of melting. In the melt ζ disappears and the entropy is maximal. Therefore the entropy increases and ζ decreases during melting. Thus $(\partial S/\partial\zeta)_{p,T}$ is negative. The correspondence between the frequency dependent heat capacity $C(\omega)$ and $\zeta(t)$ follows from

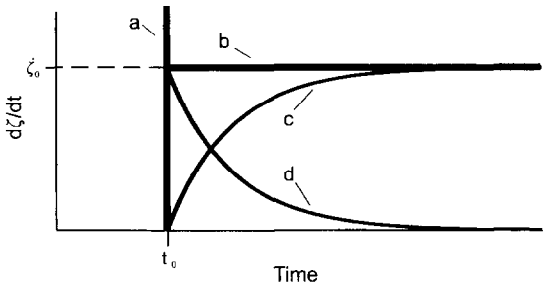

Fig. 10. The behaviour of $d\zeta/dt$ for different kinetic models. a: Model 1; b: Model 2; c: Model 3; d: Model 4 (for details see text).

Eqs. (8) and (14):

$$C(\omega) - C_{st} = \int_0^\infty \dot{C}(t)e^{-i\omega t}dt \propto -\int_0^\infty \dot{\zeta}(t)e^{-i\omega t}dt \tag{15}$$

We have to look at different kinetic models for ζ. These models are shown in Fig. 10. A discussion of the physical background will be presented elsewhere [18].

Model 1:

The melting takes place very fast (without any kinetics involved). After a temperature step ΔT_0 at the time t_0 all related crystals melt immediately. In this case ζ reads:

$$\zeta(t) = \zeta_0 - \Delta\zeta\Theta(t - t_0) \tag{16}$$

where ζ_0 describes the crystallinity before the temperature step, $\Delta\zeta$ describes the change of crystallinity relative to the small temperature change. This causes a step in the dynamic part of heat capacity as well:

$$C_{dyn}(t) = \Delta_r S_{T,p}\Delta\zeta\Theta(t - t_0) = \Delta C_0\Theta(t - t_0) \tag{17}$$

where $\Delta_r S_{T,p}$ is the partial 'entropy of reaction' (here melting) at isothermal and isobaric conditions.

Inserting of Eq. (17) into Eq. (15) yields the complex heat capacity:

$$C(\omega) = C'(\omega) = C_{st} + \Delta C_0 \tag{18}$$

This means, that for such type of transition the imaginary part C'' is zero and the real part C' is the static

heat capacity plus the frequency independent part ΔC_0. Choosing the temperature dependence of ΔC_0 this model describes the measured second-order transition (Fig. 2). It is, however, different from the measured melting curves of polymers.

Model 2:

This is a simple kinetic model, that is, after a temperature step the crystallinity changes. In a short time interval (given by the time scale of the process) the melting rate should be constant. The respective time scale in the modulated experiment is in the order of t_p. In this case the time derivation of ζ reads:

$$\dot{\zeta}(t) = -\dot{\zeta}_0 \Theta(t - t_0) \tag{19}$$

where $\dot{\zeta}_0$ ($\dot{\zeta}_0 > 0$) is the constant rate of ζ during melting. The frequency dependent heat capacity is proportional to the Fourier-transform of Eq. (19). The real part reads

$$C'(\omega) = C_{st} \tag{20}$$

and the imaginary part is

$$C''(\omega) \propto \frac{\dot{\zeta}_0}{\omega} \tag{21}$$

This kinetic model yields a constant C', which contains no information about the transition. C'' is positive and proportional to the rate of melting. This is in correspondence to the measured C'' behaviour in the melting peak region of PET and PCL.

An other result is that $\omega_0 C''$ should be constant at constant $\dot{\zeta}_0$. Because $\dot{\zeta}_0$ is dependent on the temperature, the prediction of this model is that the area of the C''-peak times ω_0 is constant (measured at the same underlying heating rate). To check this prediction, the $\omega_0 \int c'' \mathrm{d}T$ versus ω_0 diagram was plotted for PET. Fig. 11 shows the good consistency between model and measurements.

Model 3:

In principle, Model 2 describes the measured C'' curve. However, the C' should be constant, which is in contrast to the experimental results (Figs. 3–6). Therefore this model must be expanded with an additional kinetic process: the constant rate $\dot{\zeta}_0$ does not appear instantaneously but with a relaxation process:

$$\dot{\zeta}(t) = -\dot{\zeta}_0 (1 - \mathrm{e}^{-t/\tau}) \tag{22}$$

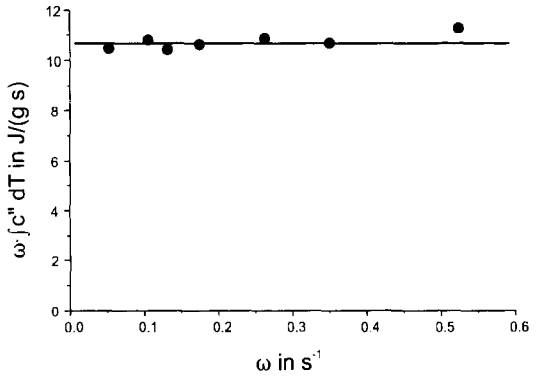

Fig. 11. Frequency dependence of the c''-peak area times ω; for details see text (measuring parameters the same as in Fig. 3).

In this case the real part C' must increase during the melting process:

$$C'(\omega) - C_{st} \propto -\dot{\zeta}_0 \frac{\tau}{1 + \omega^2 \tau^2} \tag{23}$$

and the imaginary part C'' reads:

$$C''(\omega) \propto \dot{\zeta}_0 \left(\frac{1}{\omega} - \frac{\omega \tau^2}{1 + \omega^2 \tau^2} \right) \tag{24}$$

Eq. (24) describes a positive monotone decreasing function. The changing of both C' and C'' is proportional to the melting rate. The peak height of the C''-peak as well as the C'-exothermic decreases with increasing ω. A comparison of Eqs. (23) and (24) with the experimental results shows that this model is useful for a qualitative description of the melting curves of PCL (Figs. 5 and 6). The reason for such a kinetics is local relaxation processes of the thermodynamic properties in the melt close to the crystal surface.

Model 4:

In contrast to PCL, PET shows an increase of C' in the melt region. This endothermic in C' starts at lower temperatures as the melting peak in the C_β signal and is not connected to a phase shift. C'' is relatively low. At relatively low temperatures a melting process occurs in PET which responses in phase to the temperature change (C'-curve). Such processes could be described using Model 1. In contrast to this model the experiment shows a frequency dependence of the C' signal. This behaviour must be explained by an

influence of a kinetics. A useful function for modelling such a behaviour is the exponential function

$$\dot{\zeta}(t) = -\frac{\Delta\zeta}{\tau}e^{-t/\tau} = -\dot{\zeta}_0 e^{-t/\tau} \tag{25}$$

In this case the complex heat capacity reads:

$$C'(\omega) - C_{st} \propto \dot{\zeta}_0 \frac{\tau}{1+\omega^2\tau^2} \tag{26}$$

and

$$C''(\omega) \propto \dot{\zeta}_0 \frac{\omega\tau^2}{1+\omega^2\tau^2} \tag{27}$$

In consistence with the experimental results (Fig. 3) Eqs. (26) and (27) yield endothermic (positive) effects in C' and a smaller positive peak in C''. A better correspondence would be given by a combination of this model with Model 2. In this case we must assume simultaneously melting of different types of crystals with different kinetics. This corresponds to the complicated structure of partial crystalline polymers.

5. Conclusions

The interpretation of the frequency dependent complex heat capacity $C(\omega)$ is one of the problems of the TM-DSC. $C(\omega)$ can be described using a time dependent variable ζ. The variable ζ represents the kinetic of the melting process. The knowledge of the time dependent internal variable ζ allows the interpretation of the measured curves. This is shown for polymer melting using four different models. With a combination of the presented models the experimental curve could be described qualitatively. The simultaneous presence of different kinetic processes during polymer melting is caused by the real structure of such polymers, which contains non-equilibrium crystals as well as amorphous material resulting in complicated local processes during melting close to the surfaces of the crystals. This is an additional information that is available from TM-DSC experiment.

Acknowledgements

The author gratefully acknowledges discussions with G.W.H. Höhne (University Ulm), the support of the Perkin-Elmer Corporation and G.A. van Ekenstein (University Groningen) for providing the PCL samples.

References

[1] M. Reading, D. Elliott and V.L. Hill, J. Thermal. Anal., 40 (1993) 949.
[2] P.S. Gill, S.R. Sauerbrunn and M. Reading, J. Thermal. Anal., 40 (1993) 931.
[3] J.M. Hutchinson and S. Montserrat, Thermochim. Acta, (1997) in press.
[4] J.E.K. Schawe, Thermochim. Acta, 271 (1996) 127.
[5] J.E.K. Schawe, Thermochim. Acta, 261 (1995) 183.
[6] J.M. Hutchinson and S. Montserrat, J. Thermal. Anal., 47 (1996) 103.
[7] A. Hänsel, J. Dobbertin, J.E.K. Schawe, A. Boller and C. Schick, J. Thermal. Anal., 46 (1996) 935.
[8] J.E.K. Schawe, J. Thermal. Anal., 47 (1996) 475.
[9] J.E.K. Schawe in preparation.
[10] A. Toda, T. Oda, M. Hikosaka and Y. Saruyama, Polymer, 38 (1997) 231.
[11] J.E.K. Schawe and G.W.H. Höhne, J. Thermal Anal., 46 (1996) 893.
[12] J.E.K. Schawe and G.W.H. Höhne, Thermochim. Acta, 287 (1996) 213.
[13] J.E.K. Schawe, Thermochim. Acta, this issue.
[14] J.E.K. Schawe and W. Winter, The influence of heat transfer on temperature modulated DSC measurements Thermochim. Acta, in press.
[15] J.E.K. Schawe et al. in preparation.
[16] J.E.K. Schawe, Thermochim. Acta, 229 (1993) 69.
[17] G.L. Janz, F.J. Kelly and J.L. Pérano, J. Chem. Eng. Data, 9 (1964) 133.
[18] G. Strobl and J.E.K. Schawe, Polymer, submitted.